Structure and Physical Properties of the Tetraphenylphosphonium−[Ni(dmit)$_2$]$_3$ (dmit = 2-Thioxo-1,3-dithiol-4,5-dithiolate) Salt

Takayoshi Nakamura,*,†,& Allan E. Underhill,‡ A. Treeve Coomber,§ Richard H. Friend,§ Hiroyuki Tajima,|| Akiko Kobayashi,|| and Hayao Kobayashi⊥

Research Institute for Electronic Science, Hokkaido University, Sapporo 060, Japan, Department of Chemistry, University College of North Wales, Bangor, Gwynedd LL57 2UW, U.K., Cavendish Laboratory, University of Cambridge, Madingley Road, Cambridge CB3 0HE, U.K., Department of Chemistry, Faculties of Science, The University of Tokyo, 7-3-1, Hongo, Bunkyo-ku, Tokyo 113, Japan, and Toho University, Funabashi, Chiba 274, Japan

Received July 15, 1994[⊗]

Crystals of TPP-Ni[(dmit)$_2$]$_3$ (TPP = tetraphenylphosphonium, dmit = 2-thioxo-1,3-dithiol-4,5-dithiolate) were prepared. The structure of the crystal was determined as follows: monoclinic $C2/c$; a = 18.086(3) Å, b = 7.184-(2) Å, c = 45.838(6) Å, β = 92.59(1)°, V = 5950(2) Å^3, and Z = 4. In the crystal, the large countercations separate the conducting sheet of Ni(dmit)$_2$ anions. Within the conducting sheet, two of the three Ni(dmit)$_2$ anions form columns, and remaining the Ni(dmit)$_2$ anion fills the spaces between the columns. The molecular plane of the Ni(dmit)$_2$ anions in the column is almost perpendicular to that of isolated Ni(dmit)$_2$. The electrical conductivity was nearly one-dimensional with the highest conductivity being observed parallel to the column direction. The inplane anisotropy of the conductivity was ca. 1:100. The crystal exhibited a conductivity of 10 S/cm at room temperature and semiconducting behavior at lower temperatures. Activation energies of 0.035 and 0.046 eV, respectively, were observed below and above 125 K. A deviation from Arrhenius behavior was observed above 160 K. The effect of pressure was relatively small. The crossover point between the two semiconducting regimes shifted to 80 K at 7 kbar and the activation energies decreased to 0.011 and 0.036 eV, respectively. The thermoelectric power was negative at room temperature in the column direction and showed an activation-type behavior with the crossover point around 125 K. Analysis of the reflectance spectra of the salt indicated that the gap was smaller than 0.09 eV, which is consistent with that of conductivity measurements and that the crystal is not exactly one-dimensional. The magnetic susceptibility obeyed the Curie−Weiss law below room temperature and one spin per three Ni(dmit)$_2$ units was calculated from the Curie constant. The distribution of electrons in the crystal is discussed.

Introduction

Molecular crystals of organic conductors have been intensively studied, and the solid state properties of these molecular crystals are often examined in terms of one-dimensional conductors, photoconductors, or superconductors.[1] The molecular systems of such materials are also interesting from the viewpoint of the construction of molecular devices.[2]

To achieve the desired properties in crystals or molecular systems, the regulation of the molecular arrangement is essential. The conduction properties of the materials are strongly affected by the stacking mode of donors and acceptors in the crystal. The cation radical salts of ET (bis(ethylenedithio)tetrathiafulvalene) show a polymorphism depending on the preparation conditions and with conduction properties, which range from semiconductor to superconductor with the same counteranion.[3] The arrangement of two-dimensional intermolecular interactions in the crystal are also important in obtaining metallic or superconducting salts. The molecular crystals usually show one-dimensional conduction properties due to the highly anisotropic π-orbital, which extends over the planar molecules forming the conducting sheets. To suppress metal−insulator transitions such as the Peierls transition at low temperatures a greater-than-one-dimensional Fermi surface is necessary through two-dimensional intermolecular interactions.[4]

The metal−dmit (dmit = 2-thioxo-1,3-dithiol-4,5-dithiolate) complexes are one of the candidates for obtaining two-dimensional molecular interactions.[5] The stacking mode of the metal−dmit complexes in the solid is strongly affected by the type of countercations in the crystal. Typically, columnar structures with strong intercolumn interactions are exhibited in the highly conducting salts, some of which are superconductors.[6] The spanning-overlap type of interactions seen in α-Me$_2$Et$_2$-[Ni(dmit)$_2$] results in two-dimensional conduction in the crystal.[7]

† Hokkaido University.
‡ University College of North Wales.
§ University of Cambridge.
|| The University of Tokyo.
⊥ Toho University.
& Previous address: National Institute of Materials and Chemical Research, 1-1, Higashi, Tsukuba, Ibaraki 305, Japan.
⊗ Abstract published in *Advance ACS Abstracts,* January 15, 1995.

(1) Recent progress in organic conducting materials appears in: Proceedings of International Conference on Science and Technology of Synthetic Metals. *Synth. Met.* **1993**, 55−57.
(2) (a) Proceedings of 5th International Conference on Unconventional Photoactive Solids, Symposium on Molecular Systems. *Mol. Cryst. Liq. Cryst.* **1992**, 216−218. (b) Carter, F. L. *Molecular Electronic Devices II*; Marcel Dekker, Inc.: New York and Basel, 1987. (c) Ashwell, G. J. *Molecular Electronics*, John Wiley and Sons Inc.: New York, 1992.
(3) Ferraro, J. R.; Williams, J. M. *Introduction to Synthetic Organic Conductors*, Academic Press, Inc.: Orlando, FL, 1987.
(4) Cowan, D. O.; Fortkort, J. A.; Metzger, R. M. *NATO ASI Ser. Ser. B Phys.* **1990**, *248*, 1.
(5) Cassoux, P.; Valade, L.; Kobayshi, H.; Kobayashi, A.; Clark, R. A.; Underhill, A. E. *Coord. Chem. Rev.* **1991**, *110*, 115.
(6) (a) Bousseau, M.; Valade, L.; Legros, J.-P.; Cassoux, P.; Garbauskas, M.; Interrante, L. V. *J. Am. Chem. Soc.* **1986**, *108*, 1908. (b) Kobayashi, A.; Kim, H.; Sasaki, Y.; Kato, R.; Kobayshi, H. *Chem. Lett.* **1987**, 1799. (c) Tajima, H.; Inokuchi, M.; Kobayashi, A.; Ohta, T.; Kato, R.; Kobayashi, H.; Kuroda, H. *Chem. Lett.* **1993**, 1235.

0020-1669/95/1334-0870$09.00/0

Table 1. Crystal Data for $TTP_{1/3}[Ni(dmit)_2]$

compound	$TPP[Ni(dmit)_2]_3$	V (Å^3)	5950(2)
formula	$C_{42}H_{20}Ni_3PS_{30}$	Z	4
fw	1693.49	d_{calcd} (g cm^{-3})	1.890
cryst syst	monoclinic	μ (cm^{-1})	20.2
space group	$C2/c$ (No. 15)	λ(Mo Kα) (Å)	0.710 69
a (Å)	18.086(3)	temp (°C)	21
b (Å)	7.184(2)	R[a]	0.068
c (Å)	45.838(6)	R_w[b]	0.087
β (deg)	92.59(1)		

[a] $R = \Sigma||F_o| - |F_c||/\Sigma|F_o|$ [b] $R_w = [\Sigma w(|F_o| - |F_c|)^2/\Sigma w F_o^2]^{1/2}$.

In this paper, we will describe the crystal structure of a Ni(dmit)$_2$ anion salt with the bulky countercation, TPP (tetraphenylphosphonium). The Ni(dmit)$_2$ anions stack in an unusual way in the crystal. The physical properties of the crystals associated with this extraordinary structure are examined by electrical conductivity, thermoelectric power, reflectance spectra, and magnetic susceptibility measurements.

Experimental Section

Preparation. Single crystals with the stoichiometry of $TPP_{1/3}[Ni(dmit)_2]$ were obtained by the electrocrystallization of a acetonitrile or acetonitrile-acetone mixed solution of $TPP[Ni(dmit)_2]$ and $TPP{\cdot}ClO_4$. A constant current of 1-2 μA (1.5−6 μA cm^{-1}) was applied during the crystal growth. Plate-shaped crystals with a coal-like surface were usually grown on the anode under these conditions, although platelets (typically 1.2 × 0.2 × 0.03 mm^3) were occasionally obtained from an acetonitrile−acetone mixed solution, and these were the subject of the electrical measurements.

The stoichiometry of the crystals was first determined by the elemental analysis (Found: C, 29.93; H, 1.09; N, 0.00. Calc for $C_{42}H_{20}S_{30}PNi_3$: C, 29.79; H, 1.19; N, 0.00) and was finally confirmed by X-ray analysis. The two types of crystals had identical structures by X-ray analysis.

X-ray Crystal Analysis. The X-ray data were collected on a Rigaku AFC5R four-cycle diffractometer with Mo Kα radiation (λ = 0.710 69 Å) up to 2θ = 55.2°. The cell parameters were determined from the least squares method of 2θ values using 25 reflections within the range 39.5° < 2θ < 40.5°. The crystal data are listed in Table 1. The size of the crystal used for the measurements was 0.35 × 0.35 × 0.35 mm^3. A 2θ−ω scan mode with scan width of $\omega = (0.92 + 0.30 \tan\theta)°$ and scan rate 8.0° (ω) min^{-1} was applied. A total of 10 366 reflections were collected of which 3325 reflections with $I_{obsd} > 3\sigma(I_{obsd})$ were used for the structure determination. The usual Lorentz−polarization correction was applied and correction was made for absorption (μ = 20.20 cm^{-1}). The structure was solved by the Patterson method and refined by the full-matrix least-squares method. The quantity minimized was $\Sigma w(|F_o| - |F_c|)^2$. All non-hydrogen atoms were refined anisotropically. Final R and R_w values were 0.068 and 0.087, respectively. Figure 1 shows the view of Ni(dmit)$_2$ and TPP molecules. Final atomic coordinates are listed in Table 2; main bond distances and angles in Table 3.

Electrical Measurements. Temperature-dependent electrical conductivity measurements were carried out by the ac four-probe method along the longest axis of the platelet crystal (b direction). Evaporated gold electrodes were formed on the crystal surface to which the gold wires were connected by the gold paste. The anisotropy of the conductivity was measured by the Montgomery method[8] using a platelike crystal of dimensions 1.2 × 0.2 × 0.03 mm. The electrodes were formed on the largest face of the crystal using gold paste. The crystallographic direction was determined by an automatic X-ray diffractometer. The conductivity along the third direction (c^* direction) could not be estimated by the two-probe method due to relatively high contact resistance.

The conductivity under pressure was measured using a capillary cell at up to 7 kbar. A 1:1 mixture of pentane and 2-methylbutane was used as a pressure medium. The details of the measurements have been described elsewhere.[9]

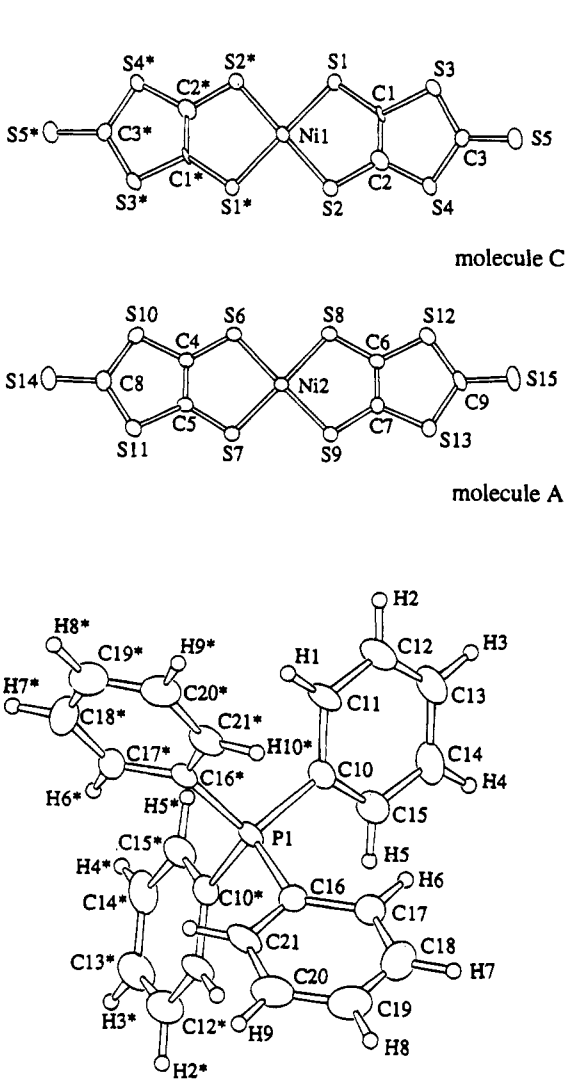

Figure 1. Perspective view of (a) Ni(dmit)$_2$ (the positions of molecules A and C are indicated in Figure 3) and (b) TPP, showing the atom-labeling scheme.

The thermoelectric power of the crystal was measured along the a^* and b axes of the platelet crystal. The samples were attached by gold paste to copper blocks through gold foil to avoid the formation of cracks in the crystal during the cooling process. The details of the measurement of thermoelectric power were reported elsewhere.[10]

Magnetic Measurements. The static magnetic susceptibility measurements were carried out by a Faraday balance. The temperature dependence was measured for crystals at a magnetic field of 0.869 and 0.766 T.

Reflectance Spectra. Polarized reflectance spectra from 5000 to 25000 cm^{-1} were measured by use of Olympus MMSP-RK microspectrophotometer[11] and spectra from 600 to 500 cm^{-1} were measured by use of Jasco IR-8900 microspectrophotometer. Optical conductivity was obtained through the modified Kramers−Krönig analysis of the reflectance spectra.[12]

Results

Crystal Structure of the Complex. The crystal has a layered structure where the conducting sheets of Ni(dmit)$_2$ anions are

(7) Kato, R.; Kobayshi, H.; Kim, H.; Kobayashi, A.; Sasaki, Y.; Mori, T.; Inokuchi, H. *Synth. Met.* **1988**, *27*, B359.
(8) Montgomery, H. C. *J. Appl. Phys.* **1971**, *42*, 2971.
(9) Guy, D. R. P.; Friend, R. H. *J. Phys. E* **1986**, *19*, 430.
(10) Miura, Y.; Takenaga, M.; Kasai, A.; Nakamura, T.; Matssumoto, M.; Kawabata, Y. *Jpn. J. Appl. Phys.* **1991**, *30*, 3503.
(11) Yakushi, K.; Iguchi, M.; Kuroda, H. *Bull. Chem. Soc. Jpn.* **1979**, *52*, 3180.
(12) Ahrenkiel, R. K. *J. Opt. Soc. Am.* **1971**, *61*, 1651.

Table 2. Positional Parameters and $B(eq)^a$ for $TPP_{1/3}[Ni(dmit)_2]^a$

atom	x	y	z	$B(eq)$ (Å^2)
Ni(1)	0	0	1/2	2.57(7)
Ni(2)	−0.22831(6)	−0.5040(3)	0.52687(3)	2.56(5)
S(1)	0.0030(2)	0.2204(5)	0.46812(7)	2.9(2)
S(2)	0.0003(2)	−0.2144(5)	0.46721(7)	3.2(2)
S(3)	0.0146(2)	0.2062(5)	0.40285(8)	3.6(2)
S(4)	0.0113(2)	−0.1963(5)	0.40195(7)	3.3(2)
S(5)	0.0324(2)	0.0067(7)	0.34707(6)	5.7(2)
S(6)	−0.3129(1)	−0.4954(6)	0.49253(6)	3.5(1)
S(7)	−0.1412(1)	−0.5075(6)	0.49653(6)	3.3(1)
S(8)	−0.3181(1)	−0.5033(6)	0.55602(6)	3.6(1)
S(9)	−0.1455(1)	0.5160(6)	0.56212(6)	3.2(1)
S(10)	−0.3048(2)	−0.4855(6)	0.42727(6)	3.7(1)
S(11)	−0.1451(1)	−0.4972(6)	0.43063(6)	3.8(1)
S(12)	−0.3197(2)	−0.5245(6)	0.62161(7)	4.3(2)
S(13)	−0.1604(2)	−0.5396(6)	0.62750(6)	5.0(2)
S(14)	−0.2260(2)	−0.4796(6)	0.37268(7)	5.3(2)
S(15)	−0.2486(2)	−0.5743(7)	0.68054(7)	6.5(2)
P(1)	1	0.1319(6)	3/4	3.0(2)
C(1)	0.0066(6)	0.097(2)	0.4367(2)	1.8(5)
C(2)	0.0068(7)	−0.096(2)	0.4355(3)	3.9(8)
C(3)	0.0195(5)	0.004(2)	0.3822(2)	3.2(4)
C(4)	−0.2641(5)	−0.489(2)	0.4623(2)	2.6(4)
C(5)	−0.1876(5)	−0.495(2)	0.4637(2)	2.8(4)
C(6)	−0.2733(5)	−0.518(2)	0.5895(2)	3.0(5)
C(7)	−0.1976(6)	−0.518(2)	0.5921(2)	3.5(5)
C(8)	−0.2259(6)	−0.487(2)	0.4086(2)	3.8(5)
C(9)	−0.2436(7)	−0.551(2)	0.6452(2)	4.1(6)
C(10)	0.9812(7)	0.280(2)	0.7808(2)	3.3(5)
C(11)	0.9191(7)	0.251(2)	0.7967(3)	4.0(6)
C(12)	0.9073(9)	0.369(3)	0.8194(3)	6.1(9)
C(13)	0.9556(9)	0.503(3)	0.8274(3)	5.7(7)
C(14)	1.0192(9)	0.536(2)	0.8117(3)	5.0(7)
C(15)	1.0304(8)	0.421(2)	0.7877(3)	4.6(7)
C(16)	1.0790(5)	−0.011(2)	0.7578(2)	3.5(5)
C(17)	1.1270(6)	0.012(2)	0.7818(2)	4.3(6)
C(18)	1.1876(9)	−0.095(3)	0.7858(4)	7(1)
C(19)	1.2020(9)	−0.235(2)	0.7659(4)	5.9(9)
C(20)	1.1539(9)	−0.264(2)	0.7422(4)	5.5(8)
C(21)	1.0923(8)	−0.159(2)	0.7384(3)	4.3(6)
H(1)	0.8841	0.1510	0.7917	4.8
H(2)	0.8620	0.3556	0.8302	7.2
H(3)	0.9458	0.5817	0.8444	6.8
H(4)	1.0548	0.6315	0.8178	6.1
H(5)	1.0729	0.4425	0.7760	5.5
H(6)	1.1169	0.1102	0.7961	5.2
H(7)	1.226	0.0728	0.8023	8.1
H(8)	1.2456	−0.3144	0.7690	6.9
H(9)	1.1657	−0.3578	0.7278	6.7
H(10)	1.0561	−0.1862	0.7223	5.5

^{a} $B(eq) = (8\pi^2/3)\sum_i\sum_j U_{ij}a_i^*a_j^*\mathbf{a}_i\cdot\mathbf{a}_j$.

separated by the layers of large counter cation (Figure 2). All the nickel atoms lie close to the $z = 0$ and $z = 1/2$ planes. The thick layers of $Ni(dmit)_2$ exist parallel to the (001) plane and are separated by TPP cations. Figure 3 shows a c-projection of the structure as well as the overlap integrals between adjacent molecules. Within a layer, the $Ni(dmit)_2$ species are arranged in an unusual way; two of the three $Ni(dmit)_2$ species form columns which stack in [010] direction (molecules A and B). The remaining $Ni(dmit)_2$ unit exists almost perpendicular to the stack (molecule C) separating adjacent columns of $Ni(dmit)_2$ dimers and has a very small interaction with adjacent monomer anions through side-by-side overlap. On the other hand, there are strong interactions between the adjacent molecules within the column. Only small interactions were observed between the isolated monomer and the column forming molecules, resulting in the highly one-dimensional nature of the crystal.

Figure 4 shows the stacking mode of the $Ni(dmit)_2$ molecules within the column. The distances between molecules are almost regular, although the pairs A−B and B−A′ overlap in a different manner. The overlap between the molecules A and B shows a

Table 3. Selected Bonding Parameters for TPP]Ni(dmit)]$_3$

	Distances (Å)		
Ni(1)−S(1)	2.157(3)	Ni(1)−S(2)	2.152(4)
Ni(2)−S(6)	2.146(3)	Ni(2)−S(7)	2.148(3)
Ni(2)−S(8)	2.149(3)	Ni(2)−S(9)	2.155(3)
S(1)−C(1)	1.70(1)	S(2)−C(2)	1.69(1)
S(3)−C(1)	1.75(1)	S(3)−C(3)	1.74(1)
S(4)−C(2)	1.70(1)	S(4)−C(3)	1.71(1)
S(5)−C(3)	1.64(1)	S(6)−C(4)	1.68(1)
S(7)−C(5)	1.69(1)	S(8)−C(6)	1.71(1)
S(9)−C(7)	1.70(1)	S(10)−C(4)	1.74(1)
S(10)−C(8)	1.71(1)	S(11)−C(5)	1.73(1)
S(11)−C(8)	1.73(1)	S(12)−C(6)	1.73(1)
S(12)−C(9)	1.72(1)	S(13)−C(7)	1.73(1)
S(13)−C(9)	1.74(1)	S(14)−C(8)	1.64(1)
S(15)−C(9)	1.63(1)	C(1)−C(2)	1.39(1)
C(4)−C(5)	1.38(1)	C(6)−C(7)	1.37(1)
P(1)−C(10)	1.81(1)	P(1)−C(16)	1.78(1)
	Angles (deg)		
S(1)−Ni(1)−S(2)	92.94(9)	S(6)−Ni(2)−S(7)	92.6(1)
S(8)−Ni(2)−S(9)	93.1(1)	Ni(1)−S(1)−C(1)	101.3(4)
Ni(1)−S(2)−C(2)	104.0(5)	C(1)−S(3)−C(3)	96.7(6)
C(2)−S(4)−C(3)	97.4(6)	Ni(2)−S(6)−C(4)	102.8(3)
Ni(2)−S(7)−C(5)	103.1(3)	Ni(2)−S(8)−C(6)	102.6(3)
Ni(2)−S(9)−C(7)	102.4(4)	C(4)−S(10)−C(8)	97.6(5)
C(5)−S(11)−C(8)	97.0(5)	C(6)−S(12)−C(9)	97.7(5)
C(7)−S(13)−C(9)	97.7(5)	C(10)−P(1)−C(10)*	108.1(8)
C(16)−P(1)−C(16)*	109.9(9)		

longitudinal offset giving a metal-over-ring arrangement. The overlap between the molecules B and A′ is a transverse offset arrangement with a longitudinal offset giving a sulfur-over-ring pattern. The interplanar distances are 3.60 and 3.58 Å between the molecules A−B and B−A′, respectively. The distances are somewhat longer than the values of 3.58 and 3.53 Å found in $(Me_4N)_{1/2}[Ni(dmit)_2]$ which shows a superconducting transition.[6]

Electrical Properties. Conductivity. The crystal shows a room-temperature conductivity of 10 S/cm along the long axis (b axis) and a semiconducting temperature dependence over the whole range measured. However, the ln(conductivity) − $1/T$ plot did not obey a single linear relationship (Figure 5). Two different linear fits were applied between 160 and 125 K and below 125 K with activation energies of 46 and 35 meV, respectively. Some deviation from linearity was observed above 160 K. The slope arownd room temperature was 3.5 meV. The behavior is similar to that reported previously for $(TPA)_{1/4}[Ni(dmit)_2]$(TPA = tetraphenylarsenium) where the activation energies were 0.03 and 0.01 eV, respectively, above and below a crossover point at 160 K.[13]

The effect of the application of a hydrostatic pressure on the conductivity behavior was small. The conductivity at room temperature increased on applying pressure and the slope of a ln(conductivity) − pressure plot was 0.05 kbar^{-1}. The semiconducting behavior was not suppressed by applying pressure up to 7 kbar, although the crossover point shifted to 80 K and the activation energies decreased to 36 and 11 meV above and below the crossover point, respectively.

The anisotropy of the in-plane conductivity was measured by the Montgomery method. The in-plane anisotropy was on the order of 1:100 with the conductivity along the longer axis (b axis) much higher than that of the shorter axis (a^* axis). The ratio of the conductivity was almost unchanged in temperature-dependent measurements. The high anisotropy in conductivity is consistent with the crystal structure where the one-dimensional $Ni(dmit)_2$ columns are separated by isolated complex.

(13) Valade, L.; Legros, J.-P.; Cassoux, P.; Kubel, F. *Mol. Cryst. Liq. Cryst.* **1986**, *140*, 335.

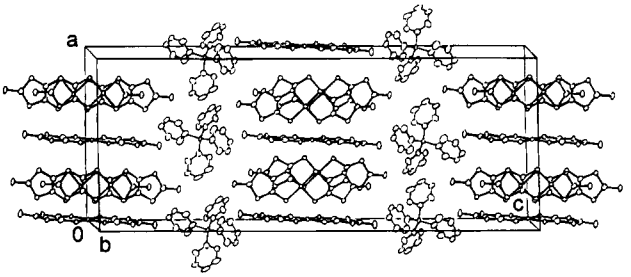

Figure 2. Crystal structure of TPP$_{1/3}$[Ni(dmit)$_2$].

Thermoelectric Power. The thermoelectric power (S) of the crystal was measured along the a^* and b axes. Figure 6 shows the $S - 1/T$ plot for the b axis measurement. An almost linear relationship was obtained below and above 125 K. The crossover point was consistent with that observed in the conductivity measurements.

The temperature dependence of S for a common semiconductor is given by

$$S = -\left(\frac{k_B}{e}\right)\left[\left(\frac{b-1}{b+1}\right)\frac{E_g}{k_BT} + \frac{3}{4}\ln\left(\frac{m_n}{m_p}\right) + \frac{b}{b-1}Q_n^* - \frac{1}{b+1}Q_p^*\right] \quad (1)$$

$$b = \frac{\mu_n}{\mu_p} \quad (2)$$

$$Q_{n,p}^* = \frac{\langle \tau_{n,p}\epsilon_{n,p}^2 \rangle}{\langle \tau_{n,p}\epsilon_{n,p} \rangle} \quad (3)$$

where m, μ, and Q are, respectively, effective mass, mobility, and heat of carrier transport.[14] τ and ϵ are scattering time and energy for carriers, respectively. By neglecting the differences in scattering times, we obtain energy gaps of 0.013 and 0.015 eV, respectively, below and above the crossover point.

The thermoelectric power along a^* axis was ca. -100 μV/K and showed almost temperature independent behavior from room temperature to 77 K. The absolute value was, however, not accurate due to the small sample size.

Magnetic Properties. The magnetic susceptibility of the polycrystalline sample showed a Curie-like behavior below room temperature. Figure 7 shows the magnetic susceptibility (χ) vs temperature. The temperature dependence was fitted by the formula,

$$\chi = \frac{C}{T - \Theta} + \chi_0 \quad (4)$$

where C, Θ, and χ_0 are the Curie constant, Weiss temperature, and diamagnetic contribution, respectively, with the values C = 0.40 emuK/mol, Θ = 1.6 K, and $\chi_0 = 3.4 \times 10^{-5}$ emu/mol. One spin per three Ni(dmit)$_2$ complexes is calculated using a value of g = 2.15 from ESR measurements. We note that with the very small value of Θ that we measure here, the exchange interactions between spins are very weak, so that the Curie law used here is indistinguishable from one-dimensional models. No anomaly in the magnetic susceptibility was observed corresponding to the crossover point obtained in the temperature dependence of the conductivity or thermoelectric power.

Reflectance Spectra. Figure 8 shows the reflectance and conductivity spectra of TPP[Ni(dmit)$_2$]$_3$. The conductivity spectra are composed of Drude-like absorption below 4000 cm^{-1}

(14) Kwak, J. F.; Beni, G.; Chaikin, P. M. *Phys. Rev. B.* **1976**, *13*, 641.

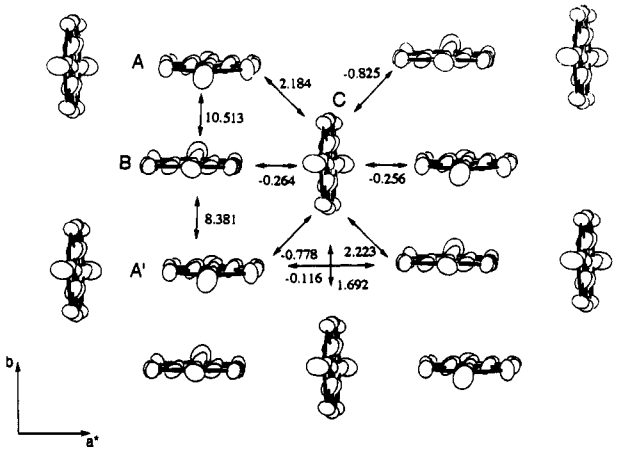

Figure 3. The c projection of TPP$_{1/3}$[Ni(dmit)$_2$] crystal together with the overlap integrals ($\times 10^3$).

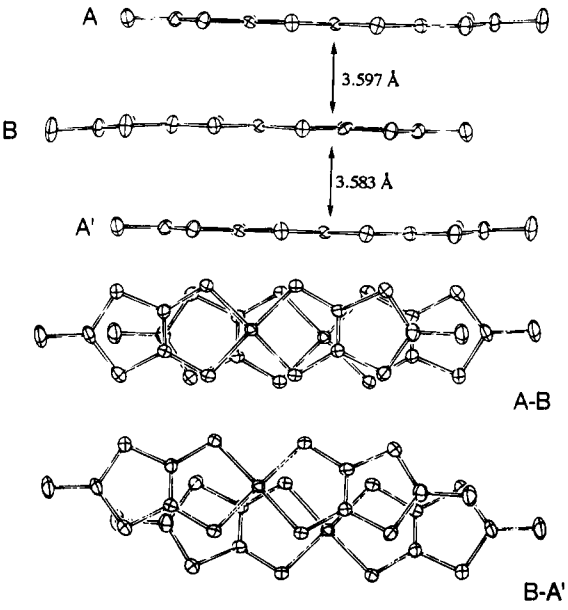

Figure 4. Stacking mode and overlap of Ni(dmit)$_2$ within the column. Molecules A, B, and A′ correspond to those indicated in Figure 2.

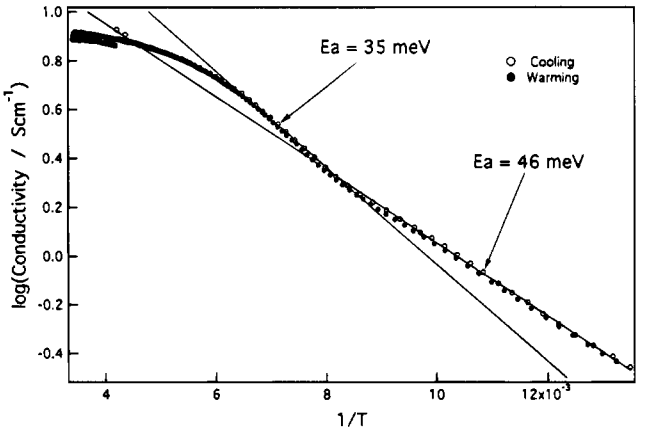

Figure 5. Temperature dependence of electrical conductivity along the b axis of TPP$_{1/3}$[Ni(dmit)$_2$]. Thin lines are the fit of Arrhenius plot.

and several vibrational transitions below 2000 cm^{-1}. The existence of the Drude-like absorption in the $E \| a$ spectra is the most striking feature in the spectra, suggesting that this salt is highly anisotropic but not quasi-one-dimensional. Considering the semiconducting properties of this salt, the Drude-like absorption is assigned to an interband transition with extremely

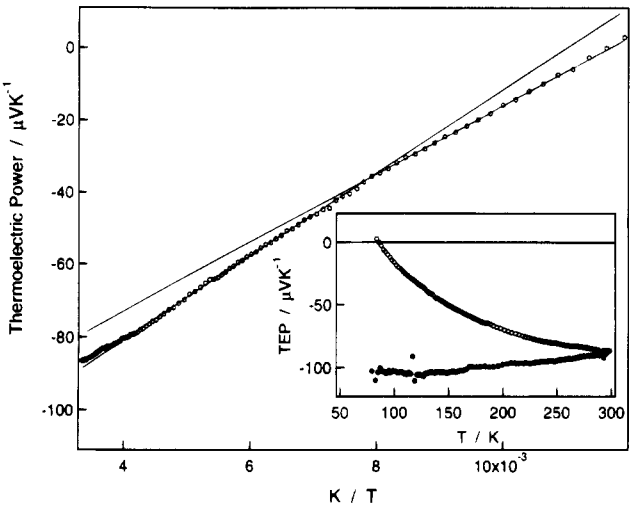

Figure 6. $S - 1/T$ plot of thermoelectric power along the b axis. Thin lines are the fit of Arrhenius plot. Inset indicates T-linear plot of thermoelectric power along the a^* and b axes.

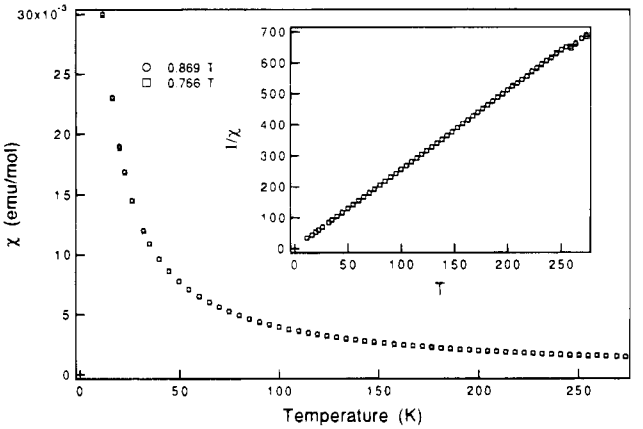

Figure 7. Temperature dependence of the magnetic susceptibility of $TPP_{1/3}[Ni(dmit)_2]$.

small optical gap ($E_g < 0.09$ eV = 700 cm^{-1}). This is consistent with the result of conductivity measurements. We calculated the plasma frequency (ω_p) of this Drude-like model by

$$\omega_p^2 = 8\int_0^{4000cm^{-1}} \sigma(\omega)\, d\omega \qquad (5)$$

and obtained $\omega_p/2\pi c = 3500$ cm^{-1} ($E \| b$) and $\omega_p/2\pi c = 1800$ cm^{-1} ($E \| a$).

In the case of highly anisotropic organic conductors, plasma frequencies are approximated by[15]

$$\omega_{p1}^2 = \frac{16e^2 d_1^2 t_1}{h^2 V_m} \sin(\pi\varrho/2) \qquad (6)$$

$$\omega_{p2}^2 = \frac{8e^2 d_2^2 t_2^2}{h^2 V_m t_1 \sin(\pi\varrho/2)} \qquad (7)$$

where V_m, ϱ, t, and d, denote the volume per molecule, charge density per molecule, transfer integral, and lattice spacing, respectively, and where subscripts 1 and 2 denote the direction parallel (1) and perpendicular (2) to the one-dimensional chain, respectively. When we assume that only the $Ni(dmit)_2$ anions forming the one-dimensional columns are actually active in the electrical conduction and therefore eqs 6 and 7 are applicable,

(15) Kwak, J. F. *Phys. Rev. B.* **1982**, *26*, 4789.

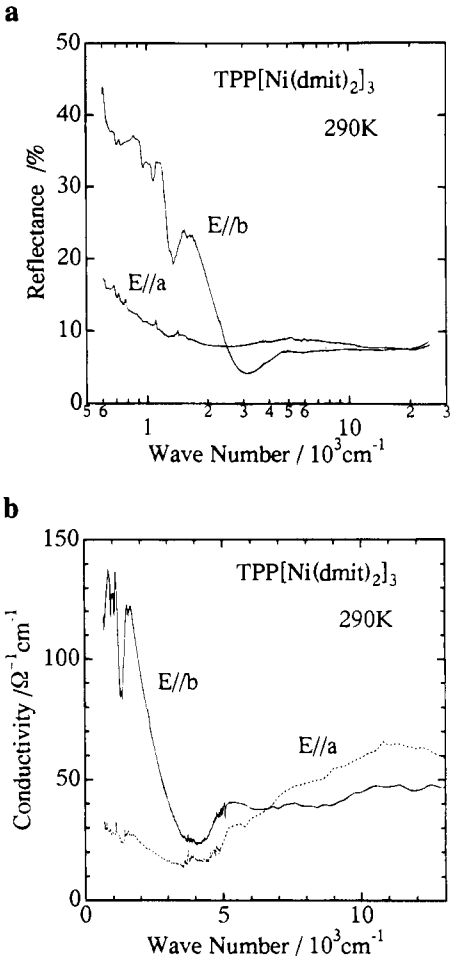

Figure 8. Reflectance (a) and conductivity (b) spectra of $TPP_{1/3}[Ni(dmit)_2]$ at 290 K.

we obtain the following relations: $t_2 = 0.014$ eV and $t_1 \sin(\pi\varrho/2) = 0.047$ eV, by use of $V_m = 5950/8$ Å^3, $d_1 = 7.184/2$ Å, $d_2 = 18.086/2$ Å, ($\omega_{p1}/2\pi c$) 3500 cm^{-1}, and ($\omega_{p2}/2\pi c$) = 1800 cm^{-1}. If we adopt the average transfer integral along conduction chain to be 0.1 eV which was obtained by extended Hückel calculation ($t = ES$: $E \approx -10$ eV), we can quite roughly estimate the charge density, ϱ, to be $\approx 1/3$.

Discussion

Closely related crystal structures with the unusual stacking mode observed in this study have been reported for $(TSF)_{1/3}[Ni(dmit)_2]$ (TSF = tetramethyltetraselenafluvalene),[16] $[Pt(dddt)_2][Ni(dmit)_2]$ (dddt^{2-} = 5,6-dihydro-1,4-dithin-2,3-dithiolate)[17] and two kinds of HMTTeF- (hexamethylenetetratellurafulvalene-) containing salts. In the crystal of $(TSF)_{1/3}[Ni(dmit)_2]$, the $Ni(dmit)_2$ units form stacks which consist of triads. The two-dimensional layers of $Ni(dmit)_2$ stacks are separated by sheets of TSF molecules, the molecular planes of which are almost perpendicular to those of $Ni(dmit)_2$ units. The crystal of $[Pt(dddt)_2][Ni(dmit)_2]$ is built up with the pairs of $Pt(dddt)_2$ units and pairs of $Ni(dmit)_2$; both of them lie perpendicularly to each other. The crystal structure of $(HMTTeF)_2[Pt(dmit)_2]$ is composed to tetradic columns of the HMTTeF which link to form a two-dimensional network.[18] The $Pt(dmit)_2$ anions are

(16) Johansen, I.; Bechgaard, K.; Rindorf, C.; Thorup, N.; Jacobsen, C. S.; Mortensen, K. *Synth. Met.* 1986, 15, 333.
(17) Faulmann, C.; Errami, A.; Legros, J.-P.; Cassoux, P.; Yagubskii, E. B.; Kotov, A. I. *Synth. Met.* **1993**, 55–57, 2057.
(18) Kobayashi, A.; Sasaki, Y.; Kato, R.; Kobayashi, H. *Chem. Lett.* **1986**, 387.

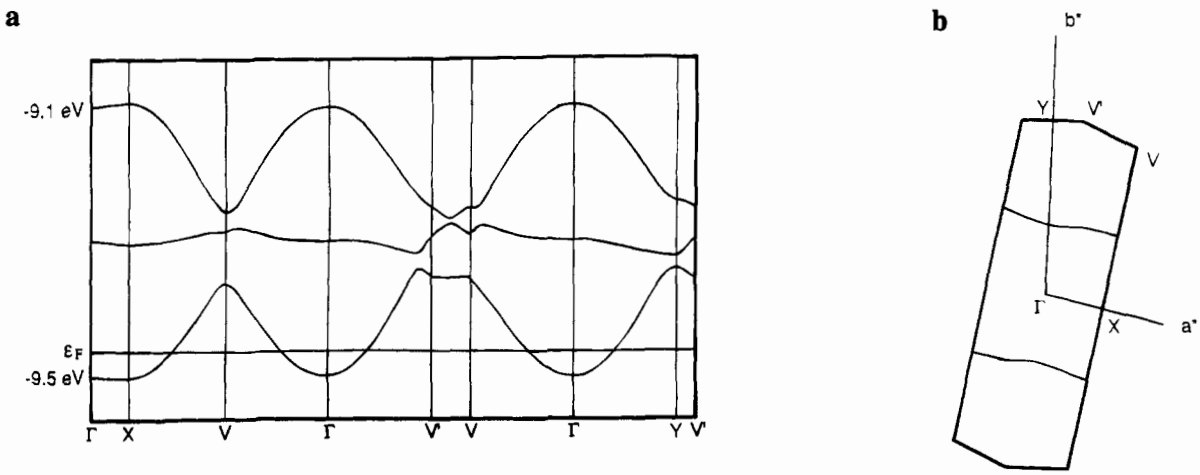

Figure 9. (a) Tight-binding band structure of TPP$_{1/3}$[Ni(dmit)$_2$]. (b) Fermi surface corresponding to Figure 8a.

located in the space between two-dimensional HMTTeF tetrad and with their molecular plane almost perpendicular to the HMTTeF molecules. In both cases, the units filling the spaces are counter cations or anions with their molecular plane perpendicular to the molecules forming conducting sheets.

In the crystal of (HMTTeF)$_4$(PF$_6$)$_2$, the conducting layer is composed of columns of HMTTeF trimers, and the remaining molecule is located between the columns with its molecular plane almost perpendicular to that of the molecules forming the columns.[19] The charges are delocalized over the three HMTTeF molecules in the column. In this case, the stacking modes observed in the crystals are probably due to the large van der Waals diameter of tellurium atom. The structure observed in the present study, however, probably owes from the effect of the large countercation.

The crystal structure and the properties of the TPA salt of Ni(dmit)$_2$ has been reported by Valade *et al.*[13] The crystal is monoclinic with the stoichiometry TPA$_{1/4}$[Ni(dmit)$_2$]. The crystal consists of Ni(dmit)$_2$ layer which are separated from each other by TPA cations. Within the layers, the Ni(dmit)$_2$ species form columns which are composed of tetrad blocks. The interplanar distances within the tetrads are 3.53 and 3.50 Å and that between tetrads is 3.76 Å. Short S···S distances between stacks are observed resulting in two-dimensional character of the conductivity. In the cation layer, empty tunnels are observed, which can be filled with variable amounts of TPA cations. As a result, variable analysis data is obtained when characterizing the various chemical phases obtained by oxidation of (TPA)[Ni(dmit)$_2$]. These results strongly suggest that the crystal structure is mainly determined by the stacks of Ni(dmit)$_2$ anions.

In the present system, in contrast to TPA salt described above, no space was observed in the cation layers, and this could be one of the reasons why such an unusual stacking mode of Ni(dmit)$_2$ anion is observed in the crystal structure. A slight difference in the size of counter cation strongly affects the crystal structure.

On the other hand, the behaviors of the temperature-dependent conductivities closely resemble each other, although the present system is highly anisotropic compared to the TPA salt. Nonlinear behavior in the log(conductivity) = $1/T$ plot was also observed in the Ni(dmit)$_2$ salt of a relatively large cation, TBA (tetrabutylammonium).[20] It was suggested that the nonlinear behavior in TBA salt could arise from subtle structural changes occurring on cooling or from changes in the carrier concentration associated with the electronic band structure.[20] It is most probable that the ordering of cations during the cooling process is related to the crossover around 125 K observed in the temperature-dependent conductivity of the present system.

The in-plane conductivity of the crystals at the *ab* plane is highly one-dimensional and is consistent with the crystal structure and the large overlap integrals observed along the stacking axis of Ni(dmit)$_2$ column.

The distribution of conduction electrons on the Ni(dmit)$_2$ anions is somewhat complicated. There are two independent Ni(dmit)$_2$ in the crystal, one forms a conduction column and the other is an isolated complex between columns. The distribution of the electrons should be determined by the small energy difference between the two types of complexes. Therefore, the prediction of the electron distribution from theoretical calculations is relatively difficult. The other possibility for the determination of the distribution is a direct determination of the electron distribution from the comparison of the bond lengths in each complex. This method was successful in the case of the complex of HMTTeF, where the structure of the crystal resembled that of the present system as described above.[19] The difference of the bond length between two different Ni(dmit)$_2$ complexes in TPP$_{1/3}$[Ni(dmit)$_2$] is, however, within experimental error.

We calculated the band structure by the tight-binding approximation, which is shown in Figure 9. Although the crystal is not a typical one-dimensional conductor from the analysis of the reflectance spectra, the overlap integrals along a^* axis (between isolated Ni(dmit)$_2$ and that forming column) are much smaller than those within the column. As a result, we obtain a one-dimensional band of molecules A and B. As we assume that all Ni(dmit)$_2$ molecules have the same energy, the band from molecule C exists at the center of the HOMO and LUMO band of molecules A and B. A one-dimensional Fermi surface is formed at the half-filled HOMO band of molecules A and B. The crystal shows an activation type conductivity, suggesting that a gap should be opening at the Fermi level. The calculation is consistent with the high conductivity along the *b* direction of the crystal; however, the temperature dependence of spin susceptibility may obey that of Boner-Fisher (one-dimensional Heisenberg antiferromagnetic chain) type susceptibility of the Hubbard system[21-23] in this simple model.

(19) Li, Z. S.; Matsuzaki, S.; Kato, R.; Kobayashi, H.; Kobayashi, A. Sano, M. *Chem. Lett.* **1986**, 1105.

(20) (a) Valade, L.; Bousseau, M.; Gleizes, A.; Cassoux, P. *J. Chem. Soc., Chem. Commun.* **1983**, 110. (b) Valade, L.; Legros, J.-P.; Bousseau, M.; Cassoux, P.; Garbauskas, M.; Interrante, L. V. *J. Chem. Soc., Dalton Trans.* **1985**, 783.

By introducing the effects of strong Coulomb interactions between electrons in comparison with the effects of band formation, we could formulate a consistent picture for the full set of properties. We note that the magnetic susceptibility indicated that each electron transferred to the $Ni(dmit)_2$ stacks gives the response expected for a noninteracting free spin, and we consider that this is firm evidence for strong Coulomb interactions. That the optical properties for light polarized along the *b* axis indicate the presence of "free" carriers suggests strongly that the electrons transferred to the $Ni(dmit)_2$ acceptors are confined to the stacks formed along the *b* axis, and we assume this to be so in the model outlined below. This would favour the arrangement of one-electron energy levels shown in Figure 9.

Using the formalism of a Hubbard model to introduce the Coulomb interactions, we propose that the on-site Coulomb repulsion energy, U, is greater than the bandwidth, *W*, so that there is preferentially only single occupation of each spatial quantum state. We note that this is consistent with the magnetic properties. Thus, the set of energy bands shown in Figure 9, would now be the lower of the two sets of Hubbard bands, and the occupancy of the this lower Hubbard band would extend to the top of the lower band shown in Figure 9, placing the Fermi energy at the gap between the two bands formed by the dimerisation of the $Ni(dmit)_2$ along the *b* axis. This is consistent with the semiconducting electrical properties, and we note that, in addition to the one-electron terms arising from the energy band calculation, the activation energy would contain a contribution from the nearest-neighbour Coulomb interaction, V_1. The "free carrier" optical response seen in the reflectivity measurements are also expected within this model at photon energies greater than the energy gap for conduction.

Summary and Conclusion

The preparation and the physical properties of $TPP_{1/3}Ni(dmit)_2$ have been described. The results can be summarized as follows.

(1) The $Ni(dmit)_2$ anions were arranged in an unusual way in the crystal. Two of three $Ni(dmit)_2$ anions form columns and remaining $Ni(dmit)_2$ anion fills spaces between columns with the molecular plane of the $Ni(dmit)_2$ anions in the column is almost perpendicular to that of isolated $Ni(dmit)_2$ anions.

(2) The conductivity of the crystal is 10 S/cm at room temperature along the *b* axis and is highly one-dimensional. The nonlinear behavior of the temperature-dependent conductivity resembles that of $TPA_{1/4}[Ni(dmit)_2]$, and is probably due to the anion ordering at low temperature. The effect of the applying pressure is relatively small.

(3) The thermoelectric power along the *b* axis is linear with $1/T$. The behavior is typical of the semiconductor where the valence band and the conduction band are not symmetric. A kink is observed in $S - 1/T$ plot at the same temperature as that observed for the temperature-dependent conductivity and the thermoelectric power along the a^* axis is almost temperature independent.

(4) An analysis of conductivity spectra indicates that the crystal is not exactly one-dimensional. The magnetic susceptibility obeys the Curie–Weiss law below room temperature with one spin per three $Ni(dmit)_2$ units calculated from the Curie constant.

(5) From the results of reflectance spectra, it may be suggested that the electrons are mainly distributed in the one-dimensional band of the column-forming dimers. However, the results of the magnetic susceptibility measurements indicated the localized Curie spins. The phenomena may be explained in terms of strong Coulomb interactions.

Acknowledgment. The authors are grateful to Dr. Keiichi Ikegami, Electrotechnical Laboratory for ESR measurement. They thank Dr. Kazumasa Honda, National Institute of Materials and Chemical Research, for the determination of the crystal axes of the samples for conductivity measurements.

Supplementary Material Available: Tables giving crystal data and details of structure determination, bond lengths, bond angles, anisotropic thermal parameters, and least-squares planes (11 pages). Ordering information is given on any current masthead page.

IC9408361

(21) Chaikin, P. M.; Kwak, J. F.; Epstein, A. *J. Phys. Rev. Lett.* **1979**, *42*, 1178.
(22) Mortensen, K.; Conwell, E. M.; Farbe, J. M. *Phys. Rev. B* **1983**, *28*, 5856.
(23) Bonner, J. C.; Fisher, M. E. *Phys. Rev.* **1964**, *135*, A640.